Contribution from the "Jožef Stefan" Institute,
"Edvard Kardelj" University of Ljubljana, 61000 Ljubljana, Yugoslavia

Synthesis and Crystal Structure of $(Xe_2F_{11}^+)_2NiF_6^{2-}$

Adolf Jesih, Karel Lutar, Ivan Leban, and Boris Žemva*

Received November 8, 1988

$(Xe_2F_{11}^+)_2NiF_6^{2-}$ has been prepared by the reaction between nickel difluoride, krypton difluoride, and xenon hexafluoride in anhydrous hydrogen fluoride. $(Xe_2F_{11}^+)_2NiF_6^{2-}$ crystallizes in the monoclinic space group $I2/a$ with a = 17.477 (5) Å, b = 5.384 (6) Å, c = 21.300 (8) Å, β = 102.83 (3)°, V = 1954.2 Å^3, Z = 4, and d_c = 3.792 g cm^{-3}. A structure determination using three-dimensional Mo Kα X-ray data resulted in conventional R and R_w factors of 0.070 and 0.094, respectively, for 1355 unique reflections for which $I > 3\sigma(I)$. The anion NiF_6^{2-} is essentially octahedral; Ni–F distances range from 1.77 (1) to 1.79 (1) Å. The $Xe_2F_{11}^+$ ion consists of two XeF_5 groups bridged by an additional common fluorine atom. The bridge bond lengths are 2.35 (1) and 2.21 (1) Å with a bridge angle of 140.3 (6)°. $(Xe_2F_{11}^+)_2NiF_6^{2-}$ represents the first known crystal structure of a compound with two $Xe_2F_{11}^+$ cations.

Introduction

During a study of the reaction rate in the xenon–fluorine system it was found that nickel difluoride is an excellent catalyst.[1] In the presence of nickel difluoride it is possible to synthesize xenon hexafluoride from the gaseous mixture Xe:F_2 = 1:5 with a high reaction rate even at 120 °C.[2]

Further reaction between the xenon hexafluoride formed, nickel difluoride, and additional fluorine did not take place even at temperatures up to 200 °C. On the other hand, a large range of hexafluoronickelates (IV) involving complex as well as simple cations had been isolated and characterized,[3-10] thus suggesting that hexafluoronickelates (IV) of the XeF_5^+ cation should also exist. This speculation was supported by our finding that during the photochemical synthesis of xenon fluorides in the presence of nickel difluoride as a catalyst[11] beautiful red crystals were obtained. Unfortunately, these crystals were never satisfactorily separated from the excess nickel difluoride, but it was clearly shown that they contained xenon and nickel. In an attempt to produce xenon(VI) fluoronickelates(IV) a synthetic route[12] was used similar to that employed in making $XeF_5^+AgF_4^-$. Nickel difluoride was treated with krypton difluoride (an oxidizer of extraordinary power[13]) in anhydrous hydrogen fluoride (AHF) and in the presence of fluoro base xenon hexafluoride. Two new xenon(VI) fluoronickelates(IV) were obtained $(XeF_6)_4NiF_4$ and $(XeF_6)_2NiF_4$. This paper describes the synthesis and crystal structure of the 4:1 compound.

Experimental Section

1. Apparatus and Reagents. A nickel vacuum line was used. It had a mercury diffusion pump, mechanical pump, and soda lime scrubbers (for removal of fluorine, hydrogen fluoride, and oxidizing fluorides) and was equipped with a Monel Helicoid pressure gauge (0–1500 Torr, ±0.3%) (Bristol Babcock Inc.) and nickel valves with Teflon packing. FEP reaction vessels (18-mm o.d.) equipped with Teflon valves were used for all preparations. Nickel difluoride (anhydrous powder, Alfa Ventron) was used as supplied. Krypton difluoride was prepared[14] by irradiation of a liquified mixture of fluorine and krypton with near-UV light at −196 °C. Xenon hexafluoride was prepared by the interaction of xenon with fluorine in the presence of nickel difluoride as a catalyst at 120 °C.[2] Fluorine was prepared and purified as described elsewhere.[15] Its purity was 99 ± 0.5 vol %. Additional purification was performed by photolysis (to scavenge oxygen impurity as dioxygen difluoride).[16] Xenon and krypton (each 99.99%) were used as supplied (Messer Griesheim, Linz, Austria). Anhydrous hydrogen fluoride (Kalie Chemie, Hannover, FRG) was purified as described previously[17] and then treated with krypton difluoride.

Table I. Crystallographic Data for $(Xe_2F_{11}^+)_2NiF_6^{2-}$

fw = 1115.85	space group: $I2/a$ (No. 15)
a = 17.477 (5) Å	λ = 0.71069 Å
b = 5.384 (6) Å	d_c = 3.792 g cm^{-3}
c = 21.300 (8) Å	μ = 80.78 cm^{-1}
β = 102.83 (3)°	transm coeff = 0.07–0.54
V = 1954.2 Å^3	$R(F_o)$ = 0.070
Z = 4	$R_w(F_o)$ = 0.094
T = 20 (2) °C	

2. Instrumentation. The magnetic susceptibility was measured by the Faraday method on a modified Newport Instrument magnetic balance. The powdered sample was packed into a thin-walled, screw-capped Kel-F container (4-mm o.d., 4-mm height). The weight of the sample was about 20 mg, and the temperature range was from −196 to 20 °C. X-ray powder diffraction patterns were obtained by the Debye–Scherrer method on an ENRAF apparatus (Delft, Holland) using graphite-monochromatized Cu Kα radiation. Finely powdered samples were loaded into 0.5-mm thin-walled quartz capillaries. The manipulations of the solids were done in a drybox (M. Braun, Garching, FRG). The residual impurities of water and oxygen in the atmosphere of the drybox did not exceed 1 ppm.

3. Preparation of $(Xe_2F_{11}^+)_2NiF_6^{2-}$. The reaction between nickel difluoride, krypton difluoride, and xenon hexafluoride in anhydrous hydrogen fluoride as a solvent yielded a red solid $(XeF_6)_4NiF_4$ that decomposed in a dynamic vacuum at room temperature yielding the slightly darker red diamagnetic compound $(XeF_6)_2NiF_4$[18] and xenon hexafluoride. Details of the preparation procedure are described elsewhere.[12] The reaction scheme is as follows ($n \geq 10$, $m \geq 10$, and z is the molar coefficient for the part of KrF_2 that thermally decomposes to the elements):

$$NiF_2 + nKrF_2 + mXeF_6 \xrightarrow[20\ °C]{HF}$$

$$(XeF_6)_4NiF_4 + (z+1)Kr + zF_2 + (n-z-1)KrF_2 + (m-4)XeF_6$$

$$\downarrow \text{dynamic vacuum, } 25\ °C$$

$$(XeF_6)_2NiF_4 + 2XeF_6$$

The curve obtained by plotting total weight versus time of pumping, presented in Figure 1, showed that in this system two compounds exist.

(1) Žemva, B.; Slivnik, J. *J. Inorg. Nucl. Chem. Suppl.* **1976**, 173.
(2) Žemva, B.; Slivnik, J. *Vestn. Slov. Kem. Drus.* **1972**, *19*, 43.
(3) Klemm, W.; Huss, E. *Z. Anorg. Allg. Chem.* **1949**, *258*, 221.
(4) Hoppe, R. *Angew. Chem.* **1950**, *62*, 339.
(5) Bode, H.; Voss, E. *Z. Anorg. Allg. Chem.* **1956**, *286*, 136.
(6) Bougon, R. *C. R. Hebd. Seances Acad Sci., Ser. C* **1968**, *267*, 681.
(7) Henkel, H.; Hoppe, R.; Allen, G. C. *J. Inorg. Nucl. Chem.* **1969**, *31*, 3855.
(8) Christe, K. O. *Inorg. Chem.* **1977**, *16*, 2238.
(9) Hoppe, R.; Fleischer, T. J. *Fluorine Chem.* **1978**, *11*, 251.
(10) Bougon, R.; Christe, K. O. Wilson, W. W. *J. Fluorine Chem.* **1985**, *30*, 237.
(11) Lutar, K.; Slivnik, J. Presented at the 8th European Symposium on Fluorine Chemistry, Jerusalem, Israel, 1983; *J. Fluorine Chem.* **1983**, *23*, 430.
(12) Lutar, K.; Jesih, A.; Žemva, B. *Rev. Chim. Miner.* **1986**, *23*, 565.
(13) Bartlett, N.; Sladky, F. O. The Chemistry of Krypton, Xenon and Radon. In *Comprehensive Inorganic Chemistry*; Bailar, J. C., Trotman-Dickenson, A. F., Eds.; Pergamon: Oxford and New York, 1973; Vol. I, p 245.
(14) Slivnik, J.; Šmalc, A.; Lutar, K.; Žemva, B.; Frlec, B. *J. Fluorine Chem.* **1975**, *5*, 273.
(15) Slivnik, J.; Šmalc, A.; Zemljič, A. *Vestn. Slov. Kem. Drus.* **1965**, *12*, 17.
(16) Šmalc, A.; Lutar, K.; Slivnik, J. *J. Fluorine Chem.* **1975**, *6*, 287.
(17) Booth, H. Simmons, Ed. *Inorganic Syntheses*; McGraw-Hill: New York, 1939; Vol. I, p 134.
(18) Žemva, B.; Lutar, K.; Jesih, A. To be submitted for publication.

0020-1669/89/1328-2911$01.50/0

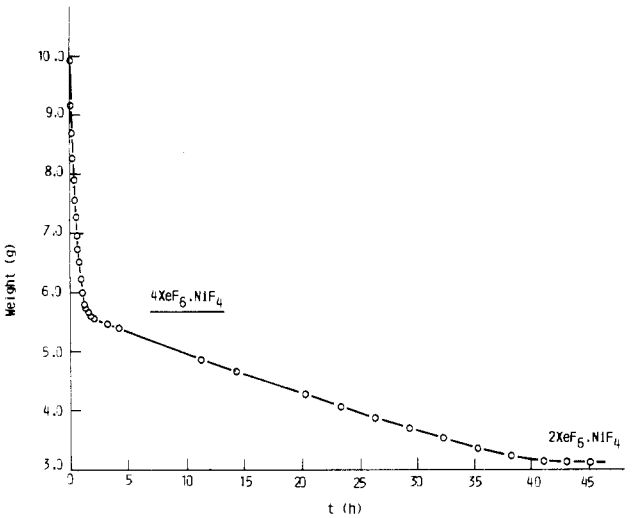

Figure 1. Dependence of the total weight of the sample on the time of pumping off volatiles in the course of $(XeF_6)_2NiF_4$ preparation at room temperature.

Table II. Atom Coordinates ($\times 10^4$) and Temperature Factors ($Å^2 \times 10^3$) for $(Xe_2F_{11}^+)_2NiF_6^{2-}$

	x	y	z	U^a
Ni	5000	0	0	33 (2)
Xe(1)	3777 (1)	3216 (2)	934 (1)	34 (1)
Xe(2)	6139 (1)	692 (3)	1650 (1)	38 (1)
F(1)	2811 (9)	3633 (26)	1097 (8)	67 (9)
F(2)	3221 (8)	745 (25)	442 (7)	55 (8)
F(3)	3340 (7)	5450 (22)	287 (7)	48 (7)
F(4)	3942 (8)	5977 (25)	1484 (7)	53 (8)
F(5)	3852 (8)	1195 (22)	1641 (6)	53 (8)
F(6)	6858 (9)	-687 (28)	2311 (7)	62 (9)
F(7)	6287 (8)	-2451 (25)	1301 (7)	53 (8)
F(8)	7061 (9)	1790 (31)	1455 (7)	63 (9)
F(9)	6327 (10)	3233 (34)	2263 (7)	74 (11)
F(10)	5478 (9)	-796 (26)	2116 (6)	57 (9)
F(11)	5121 (9)	3233 (24)	1430 (6)	54 (8)
F(12)	4462 (7)	2767 (23)	30 (5)	40 (6)
F(13)	5865 (7)	1412 (21)	447 (6)	43 (7)
F(14)	5227 (7)	913 (23)	-747 (5)	42 (7)

[a] Equivalent isotropic U defined as one-third of the trace of the orthogonalized U_{ij} tensor.

The 4:1 compound was seen to be completely stable at 0 °C but to loose xenon hexafluoride in a dynamic vacuum at room temperature with the rate of about 13 mg XeF_6/mol h, leaving the 2:1 compound, which is stable at room temperature. The vapor pressures of $(XeF_6)_4NiF_4$ at 0 °C and $(XeF_6)_2NiF_4$ at room temperature were immeasurably small.

4. Preparation of $(Xe_2F_{11}^+)_2NiF_6^{2-}$ Single Crystals. The solubility of $(Xe_2F_{11}^+)_2NiF_6^{2-}$ in anhydrous hydrogen fluoride is moderately high; therefore, the crystals were prepared directly during the preparation of the compound itself. After the preparative interaction was complete the excess of anhydrous hydrogen fluoride, xenon hexafluoride, krypton difluoride, krypton, and fluorine was pumped off at 0 °C. The red crystals remaining were loaded in 0.5-mm quartz capillaries in a drybox. Because the crystals have some dissociation pressure of xenon hexafluoride at room temperature, the manipulation in the drybox had to be quick. Also, the capillaries were carefully pretreated before use (heated for 24 h at 400 °C and exposed to elemental fluorine).

5. Structural Determination of $(Xe_2F_{11}^+)_2NiF_6^{2-}$. Out of 15 crystals mounted in specially prepared quartz capillaries, only 1 had acceptable diffractive properties. In spite of the decay (24.7% of I) it was possible to collect a set of diffraction data with a scan time of 10 s up to 2θ of 56° for Mo Kα radiation. A total of seven reflections were deleted because of excessively large discrepancies during the refinement. The crystal structure was solved by Patterson and Fourier techniques. Details of the procedures used for data collection and refinement are given in Table I (see also Table SI in the supplementary material). Atomic coordinates and temperature factors are given in Table II, and selected bond lengths and angles are in Table III.

6. Description of the $(Xe_2F_{11}^+)_2NiF_6^{2-}$ Structure. As may be seen from Figures 2 and 3 (Figures S1 and S2 in the supplementary material) and Table III, the structure analysis clearly defines an NiF_6 group and

Table III. Selected Bond Lengths[a] (Å) and Angles[a] (deg) for $(Xe_2F_{11}^+)_2NiF_6^{2-}$

		Cation[b]	
Xe(1)–F(1)	1.81 (2)	Xe(2)–F(6)	1.82 (1)
Xe(1)–F(2)	1.83 (1)	Xe(2)–F(7)	1.89 (1)
Xe(1)–F(3)	1.86 (1)	Xe(2)–F(8)	1.85 (2)
Xe(1)–F(4)	1.87 (1)	Xe(2)–F(9)	1.87 (2)
Xe(1)–F(5)	1.85 (1)	Xe(2)–F(10)	1.86 (2)
Xe(1)–F(11)	2.35 (1)	Xe(2)–F(11)	2.21 (1)
Xe(1)–F(12)	2.49 (1)	Xe(2)–F(13)	2.53 (1)
Xe(1)–F(14^i)	2.90 (1)	Xe(2)–F(14^i)	2.84 (1)
F(1)–Xe(1)–F(2)	78.5 (7)	F(6)–Xe(2)–F(7)	78.9 (6)
F(1)–Xe(1)–F(3)	79.3 (7)	F(6)–Xe(2)–F(8)	79.5 (7)
F(1)–Xe(1)–F(4)	78.6 (6)	F(6)–Xe(2)–F(9)	77.0 (7)
F(1)–Xe(1)–F(5)	79.6 (7)	F(6)–Xe(2)–F(10)	79.4 (7)
F(2)–Xe(1)–F(3)	88.1 (6)	F(7)–Xe(2)–F(8)	89.8 (7)
F(2)–Xe(1)–F(4)	157.1 (7)	F(7)–Xe(2)–F(9)	155.8 (6)
F(2)–Xe(1)–F(5)	87.9 (6)	F(7)–Xe(2)–F(10)	88.8 (6)
F(3)–Xe(1)–F(4)	86.1 (6)	F(8)–Xe(2)–F(9)	84.0 (7)
F(3)–Xe(1)–F(5)	158.9 (6)	F(8)–Xe(2)–F(10)	158.8 (6)
F(4)–Xe(1)–F(5)	89.6 (6)	F(9)–Xe(2)–F(10)	88.6 (7)
F(1)–Xe(1)–F(11)	142.5 (6)	F(6)–Xe(2)–F(11)	143.1 (6)
F(1)–Xe(1)–F(12)	141.9 (6)	F(6)–Xe(2)–F(13)	141.9 (6)
F(1)–Xe(1)–F(14^i)	137.2 (5)	F(6)–Xe(2)–F(14^i)	136.8 (5)
F(11)–Xe(1)–F(12)	75.2 (6)		
		Anion[b]	
Ni–F(12), F(12^i)	1.77 (1)	F(12)–Ni–F(13)	90.9 (5)
Ni–F(13), F(13^i)	1.77 (1)	F(12)–Ni–F(14)	91.4 (5)
Ni–F(14), F(14^i)	1.79 (1)	F(13)–Ni–F(14)	91.6 (6)
		Additional Angles[b]	
Xe(1)–F(11)–Xe(2)	140.3 (6)	Xe(1)–F(14^i)–Ni	99.8 (5)
Xe(1)–F(12)–Ni	117.3 (5)	Xe(2)–F(14^i)–Ni	101.5 (5)
Xe(2)–F(13)–Ni	115.2 (6)	Xe(1)–F(14^i)–Xe(2)	96.5 (4)

[a] Estimated standard deviations in parentheses. [b] Symmetry code: (i) $1-x, -y, -z$.

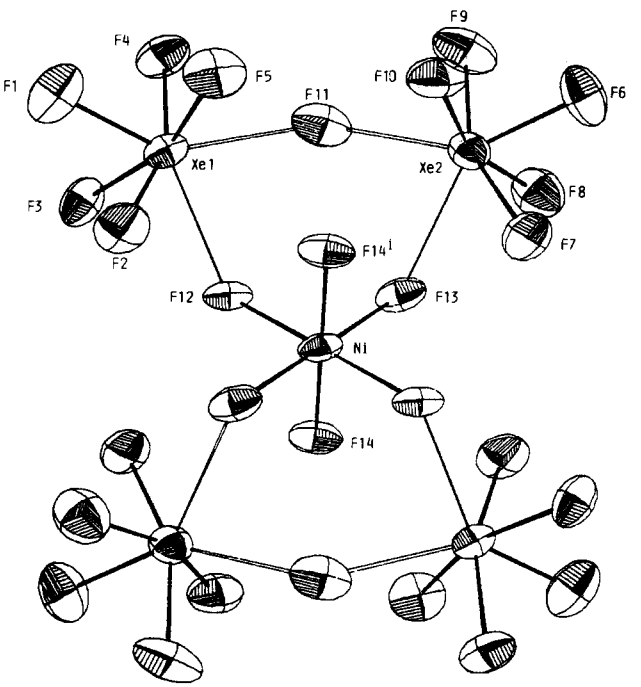

Figure 2. ORTEP diagram of $(Xe_2F_{11}^+)_2NiF_6^{2-}$.

two Xe_2F_{11} groups. The Xe_2F_{11} group consists of two similar XeF_5 groups linked by an additional common flourine atom. All four xenon atoms and the nickel atom are in the same plane, with the nickel atom representing a center of inversion.

The NiF_6 group is approximately octahedral with an average Ni–F value of 1.78 (1) Å. The cis F–Ni–F angles are close to 90°, the greatest deviations being for F(12)–Ni–F(14) = 91.4 (5)° and F(13)–Ni–F(14^i) = 91.6 (6)°.

The interatomic distances Xe(1)–F(11) and Xe(2)–F(11) in the Xe_2F_{11} group are sufficiently short (2.35 (1) and 2.21 (1) Å, respectively)

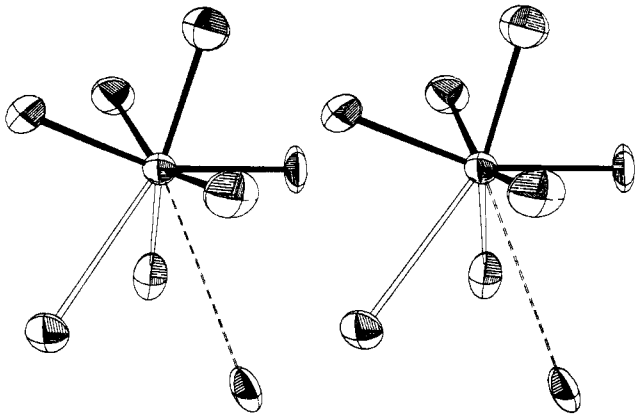

Figure 3. Stereogram showing the typical xenon coordination in fluorine atoms (exemplified by Xe(1) coordination).

to justify the formulation Xe_2F_{11} species, especially because other intergroup contacts are much longer. The Xe(1)–F(11)–Xe(2) angle is 140.3 (6)°. Both XeF_5 groups forming a Xe_2F_{11} group are crystallographically distinct, and the bridge bonding by the shared fluorine ligand (F(11)) is slightly unsymmetrical. Each XeF_5 group is approximately a square-based pyramid, with the xenon atom placed below the base. The F_{ax}–Xe–F_{eq} angles are close to 80° in both XeF_5 groups, the greatest deviation being for F(6)–Xe(2)–F(9) = 77.0 (7)°. Both XeF_5 groups depart from C_{4v} symmetry, and the cis F_{eq}–Xe–F_{eq} angles in each XeF_5 species are not equal. The smallest cis angles in both XeF_5 groups (F(3)–Xe(1)–F(4) = 86.1 (6)° and F(8)–Xe(2)–F(9) = 84.0 (7)°) are those furthest from the unshared fluorine $F(14^i)$ of the NiF_6 species.

The interatomic distances for the five F ligands bound to Xe(2) are, on a one on one comparison, longer than those for Xe(1). But the bridging F ligand (F(11)) is closer to Xe(2) than to Xe(1). As may be seen from Figure 3 and Table III, each Xe of the XeF_5 species is making a short bridging interaction with F(11) and with one F ligand of the NiF_6^{2-} (F(12) or F(13)). The two bridging F ligands, the Xe atom, and the axial F ligand of the XeF_5 group (F(1) on Xe(1) and F(6) on Xe(2)) are coplanar (thus e.g. F(1)–Xe(1)–F(11) = 142.5 (6)°, F(1)–Xe(1)–F(12) = 141.9 (6)°, and F(11)–Xe(1)–F(12) = 75.2 (6)°, and they sum to 359.6 (6)°). The interatomic distances Xe(1)–F(14) = 2.90 (1) Å and Xe(2)–F(14) = 2.84 (1) Å represent the next closest Xe atom to F ligand contact. These are contacts between adjacent formula units and simply arise from close packing of those units. There is no clear evidence of directed bonding in those interactions.

Results and Discussion

A large set of complexes of general formula $(XeF_6)_4MF_4$ (M = Ce,[19] Pr,[19] Tb,[19] Ti,[20] Mn,[21] Pd,[22] Ge,[23] Sn,[24,25] and Pb[25]) is known. Although in fluoronickelates the oxidation state 4+ is readily obtained,[3] no evidence for the formation of a xenon(VI) fluoronickelate(IV) was found in the course of studies of the reaction between nickel difluoride, xenon hexafluoride, and fluorine under pressure.[1] It appeared that xenon hexafluoride was not a sufficiently strong base to stabilize Ni^{4+} at higher temperatures (above 200 °C) where otherwise[3] the oxidation of Ni^{2+} to Ni^{4+} could occur. To offset possible low thermal stability of the XeF_6/NiF_4 complexes, krypton difluoride was used as a fluorinating and oxidizing agent and the reaction was performed at room temperature. A red diamagnetic solid was obtained, which proved to be unstable in a dynamic vacuum at room temperature. This first product, $(XeF_6)_4NiF_4$, lost xenon hexafluoride slowly, forming a 2:1 compound.

The crystal structure of $(XeF_6)_4NiF_4$ confirms the earlier speculation[26] that complexes of the type $(XeF_6)_4MF_4$ are $Xe_2F_{11}^+$ salts. A low-spin $d_{t_{2g}}^6$ Ni(IV) electron configuration is anticipated to be akin to the configurations of Pt(IV) and Pd(IV) and like them to favor a regular octahedral MF_6 species. The cis angles of the anion F(12)–Ni–F(14) = 91.4 (5)° and F(13)–Ni–$F(14^i)$ = 91.6 (6)° show that NiF_6^{2-} is not perfectly octahedral but is slightly distorted as a consequence of interaction with the $Xe_2F_{11}^+$ cations. The average Ni–F distance of 1.78 (1) Å agrees well with the Ni–F distance of 1.78–1.79 Å evaluated by Hoppe[9] for the series of complexes M_2NiF_6 (M = K, Rb, Cs, or a mixture of these elements) and the Ni–F distance of 1.776 (8) Å determined in K_2NiF_6 by a neutron diffraction powder analysis.[27]

The cation $Xe_2F_{11}^+$ was crystallographically defined first[26] in the compound $Xe_2F_{11}^+AuF_6^-$. The crystal structure of $(Xe_2F_{11}^+)_2NiF_6^{2-}$ represents the first example of two $Xe_2F_{11}^+$ cations linked to the same anion. Comparison of $(Xe_2F_{11}^+)_2NiF_6^{2-}$ with $Xe_2F_{11}^+AuF_6^-$ reveals a greater interaction of the cation with the anion in the former. This is evident from the significantly smaller angle between both XeF_5 units and the bridging fluorine of the complex cation, which is 169.2 (2)° in the case of the gold compound and only 140.3 (6)° in the case of the nickel compound. The stronger cation–anion interaction in the nickel salt is probably a result of the large average negative charge on the fluorine ligands of NiF_6^{2-}. The closer approach of the anion ligands to the xenon atoms in the nickel salt may be the cause of a slightly large average Xe–F bridging distance in that case in comparison with $Xe_2F_{11}^+AuF_6^-$. The bridge bonding in both cations of the nickel compound is slightly asymmetrical. The xenon atom that has, on average, the longer bonds in its XeF_5 unit has the shorter bridge bond. This is consistent with the view that the closer the bridging fluorine ligands to a XeF_5 entity then the more xenon hexafluoride like it becomes.

The $Xe_2F_{11}^+$ cation can therefore be described as a resonance hybrid of canonical forms $(XeF_5^+F^-XeF_5^+)$, $(XeF_6XeF_5^+)$, and $(XeF_5^+XeF_6)$, the last two being of unequal weight. Evidently the ligand charge on NiF_6^{2-} is just low enough to allow the xenon hexafluoride base to displace the anion ligands in $(XeF_5^+)_2NiF_6^{2-}$ from their interaction with XeF_5^+, so forming the $Xe_2F_{11}^+$ salt. As was already mentioned, $(Xe_2F_{11}^+)_2NiF_6^{2-}$ is quite unstable and easily looses xenon hexafluoride, forming only $(XeF_5^+)_2NiF_6^{2-}$.

All four XeF_5 groups of the two $Xe_2F_{11}^+$ species resemble the cations in XeF_5^+ salts.[22] Xe–F_{ax} is 1.81 (2) and 1.82 (1) Å, respectively, being shorter than the average Xe–F_{eq} bond length, which is 1.86 Å. As in $Xe_2F_{11}^+AuF_6^-$ and the complex $XeF_2XeF_5^+AsF_6^-$,[28] each XeF_5 unit in $(Xe_2F_{11}^+)_2NiF_6^{2-}$ is interacting strongly with two F ligands. In $(Xe_2F_{11}^+)_2NiF_6^{2-}$ one of these is the bridging fluorine ligand. It seems that the coordination geometry of each XeF_5 group and its two bridging ligands is determined by simple Coulombic interactions. These involve the negatively charged bridging F, the somewhat negative equatorial ligands of the XeF_5 group, and the positive charge on the xenon atom. The latter is shielded on the pseudo 4-fold axis (trans to the axial F ligand) by the nonbonding xenon valence-electron pair. The observed geometry nicely conforms to the balance of these repulsive and attractive interactions. The axial F ligand of the XeF_5, the xenon atom, and the two bridging F ligands are coplanar. Each bridging F is so disposed for most favorable interaction with the positive charge at the xenon (shielded as it must be by the sterically active nonbonding valence-electron pair). At the same time the equatorial ligands of the XeF_5 groups are placed as far away from the bridging ligands as possible and are in consequence placed symmetrically above and below the plane defined by the Xe atom and the two bridging F ligands.

Acknowledgments. We gratefully acknowledge support of the U.S.-Yugoslav Joint Fund for Scientific and Technological cooperation, in cooperation with the National Science Foundation

(19) Družina, B.; Lutar, K.; Žemva, B. Presented at the International Symposium "Centenary of the Discovery of Fluorine", Paris, 1986; paper I-10.
(20) Žemva, B.; Slivnik, J.; Bohinc, M. *J. Inorg. Nucl. Chem.* **1976**, *38*, 73.
(21) Bohinc, M.; Grannec, J.; Slivnik, J.; Žemva, B. *J. Inorg. Nucl. Chem.* **1976**, *38*, 75.
(22) Leary, K.; Templeton, D. H.; Zalkin, A.; Bartlett, N. *Inorg. Chem.* **1973**, *12*, 1726.
(23) Pullen, K. E.; Cady, G. H. *Inorg. Chem.* **1967**, *6*, 1300.
(24) Pullen, K. E.; Cady, G. H. *Inorg. Chem.* **1966**, *5*, 2057.
(25) Žemva, B.; Jesih, A. *J. Fluorine Chem.* **1984**, *24*, 281.
(26) Leary, K.; Zalkin, A.; Bartlett, N. *Inorg. Chem.* **1974**, *13*, 775.
(27) Taylor, J. C.; Wilson, P. W. *J. Inorg. Nucl. Chem.* **1974**, *36*, 1561.
(28) Žemva, B.; Jesih, A.; Templeton, D. H.; Zalkin, A.; Cheetham, A. K.; Bartlett, N. *J. Am. Chem. Soc.* **1987**, *109*, 7420.

under Grant No. 552 and the Research Community of Slovenia.

Registry No. $(Xe_2F_{11}^+)_2NiF_6^{2-}$, 121125-44-8.

Supplementary Material Available: For $(Xe_2F_{11}^+)_2NiF_6^{2-}$, Tables SI and SII, listing full crystal data and details of structure determination and refinement and anisotropic temperature factors, and Figures S1 and S2, showing ORTEP stereograms of the compound and its unit-cell contents (5 pages); Table SIII, listing observed and calculated structure factors (8 pages). Ordering information is given on any current masthead page.

Contribution from the Department of Chemistry, University of New Mexico, Albuquerque, New Mexico 87131, and Central Research and Development Department,[§] Experimental Station, E. I. du Pont de Nemours & Company, Wilmington, Delaware 19898

Encapsulation of Lead Sulfide Molecular Clusters into Solid Matrices. Structural Analysis with X-ray Absorption Spectroscopy

Karin Moller,[†] Thomas Bein,*[,†] Norman Herron,[‡] Walter Mahler,[‡] and Ying Wang[‡]

Received December 19, 1988

Molecular-size PbS species have been stabilized in the open-pore structure of zeolite Y and mordenite via ion exchange with Pb(II) and subsequent treatment with H_2S at 295 K. Detailed analysis of synchrotron X-ray absorption data of the Pb L_{III}-edge shows that intrazeolite $PbO_2(O_z)_3$ (O_z = zeolite oxygen) species in zeolite Y react with H_2S to form monomolecular $S_2Pb(O_z)_3$ species that are still anchored to the zeolite framework. The intrazeolite PbS phase appears to be more ordered at high loading levels of lead in zeolite Y than at low loading levels. The coordination of Pb(II) and the structure of PbS in the mordenite host is less ordered but basically very similar to that of the monomolecular species in Y. Optical absorption data for these samples agree very well with the structural EXAFS results. Larger PbS clusters have been stabilized in 85% ethylene–15% methacrylic acid copolymer films by a similar preparation procedure. EXAFS data indicate that the reaction forms PbS clusters with several Pb coordination shells and that the conversion of PbS is a function of Pb(II) loading levels.

Introduction

Quantum size effects in small semiconductor particles have been known for two decades.[1] The majority of investigations have been performed on colloids in solution, which are often subject to aggregation even if stabilizers are added.[2-4] Attempts to overcome this problem are typically based upon arrested precipitation via incorporation of the semiconductor particles in more rigid environments such as glasses, micelles, polymers, or recently lipid membranes.[5] When semiconductor particle dimensions are reduced, a blue shift in the absorption spectra relative to that of the bulk is generally observed. This shift is strongly dependent upon the particle size. Recently, we have shown that zeolites are useful hosts for stabilizing extremely small clusters of CdS and CdSe. These clusters, which are well-defined arrangements of only a few atoms, still exhibit exciton peaks in the electronic absorption spectra, characteristic for the bulk materials.[6-8] The present contribution describes an extension of these studies to the encapsulation of lead sulfide clusters in zeolites and, for comparison, in a polymer matrix. The optical properties of these CdS and PbS clusters in zeolite and polymer composites were reported earlier.[9,10] The dependence of the band gap on PbS cluster size has been extensively studied by using PbS particles embedded in methacrylic acid copolymer.[11] A dramatic blue shift of the absorption edge from 3200 nm for bulk PbS samples to 530 nm was shown to occur upon decreasing the particle size. The lower size limit of the PbS clusters was estimated to be smaller than 13 Å by comparing the discrete features in the absorption spectra with similar spectra of CdS clusters stabilized in zeolite hosts with similar framework cavities. Here we report on the structural characteristics of PbS species in a variety of solid supports that, in principle, impose different spatial confinement on the growth of the semiconductor clusters. The structural information was derived from the analysis of EXAFS (extended X-ray absorption fine structure) data for the lead L_{III} absorption edge.

Experimental Section

Lead(II) cations were exchanged into zeolites Y (Linde LZ-Y52) and mordenite (Linde LZ-M5) from an aqueous solution of $Pb(NO_3)_2$ at room temperature. The zeolite samples were subsequently dehydrated by slowly heating up to 673 K under a flow of oxygen. After cooling to ambient temperature, all samples were treated with hydrogen sulfide

Table I. Sample Compositions of Lead-Containing Zeolites and Polymers

matrix	sample name	stoichiometry/compn
zeolite Y	PbY24	$Pb_{24.4}Na_{1.8}Al_{48}Si_{144}O_{384}$
	PbSY24	$Pb_{24.4}S_{11.2}Na_{1.8}Al_{48}Si_{144}O_{384}$
	PbSY1	$Pb_{1.1}S_{1.5}Na_{43}Al_{46}Si_{146}O_{384}$
mordenite	PbM3	$Pa_{3.1}Na_{0.8}Al_8Si_{40}O_{96}$
	PbSM3	$Pb_{3.1}S_{1.2}Na_{0.8}Al_8Si_{40}O_{96}$
polymer (E-MAA)	PbP20	20 wt % Pb, 2.5 mg/cm^2
	PbP2	2.0 wt % Pb, 0.25 mg/cm^2
	PbSP24	24 wt % PbS, 3 mg/cm^2
	PbSP2.4	2.4 wt % PbS, 0.3 mg/cm^2

Table II. Crystallographic Data for Reference Samples and Their Utilization in the EXAFS Analysis

	EXAFS Fourier transform ranges		crystallographic data		
ref compd	k/Å^{-1}	R/Å	R/Å	N	ref
$Pb(NO_3)_2$					
Pb–O	2.7–14.6	1.5–2.6	2.81	12	22
Pb–O			4.45, 4.76, 4.89	3 × 6	
Pb–N			3.22	6	
Pb–Pb			5.55	12	
PbS					
Pb–S	3.2–14.6	1.9–3.0	2.97	6	23
Pb–Pb	3.2–14.6	3.5–4.5	4.20	12	
Pb–S			5.14	8	
Pb–Pb			5.94	6	

(1) Berry, C. R. *Phys. Rev.* **1967**, *161*, 848.
(2) Rosetti, R.; Nakahara, S.; Brus, L. E. *J. Chem. Phys.* **1983**, *79*, 1086.
(3) Fojtik, A.; Weller, H.; Koch, U.; Henglein, A. *Ber. Bunsen-Ges. Phys. Chem.* **1984**, *88*, 969.
(4) Ramsden, J. J.; Webber, S. E.; Grätzel, M. *J. Phys. Chem.* **1985**, *89*, 2740.
(5) Zhao, X. K.; Baral, S.; Rolandi, R.; Fendler, J. H. *J. Am. Chem. Soc.* **1988**, *110*, 1012.
(6) Herron, N.; Wang, Y.; Eddy, M. M.; Stucky, G. D.; Cox, D. E.; Moller, K.; Bein, T. *J. Am. Chem. Soc.* **1989**, *111*, 530.
(7) Wang, Y.; Herron, N. *J. Phys. Chem.* **1988**, *92*, 4988.
(8) Moller, K.; Eddy, M. M.; Stucky, G. D.; Herron, N.; Bein, T. *J. Am. Chem. Soc.* **1989**, *111*, 2564.

[†] University of New Mexico.
[‡] E. I. du Pont de Nemours & Co.
[§] Contribution No. 5008.

0020-1669/89/1328-2914$01.50/0